Clim Dyn (2014) 43:2333–2348
DOI 10.1007/s00382-014-2056-1

A multi-model comparison of Atlantic multidecadal variability

Jin Ba · Noel S. Keenlyside · Mojib Latif · Wonsun Park · Hui Ding · Katja Lohmann · Juliette Mignot · Matthew Menary · Odd Helge Otterå · Bert Wouters · David Salas y Melia · Akira Oka · Alessio Bellucci · Evgeny Volodin

Received: 26 July 2013 / Accepted: 13 January 2014 / Published online: 30 January 2014

Abstract A multi-model analysis of Atlantic multidecadal variability is performed with the following aims: to investigate the similarities to observations; to assess the strength and relative importance of the different elements of the mechanism proposed by Delworth et al. (J Clim 6:1993–2011, 1993) (hereafter D93) among coupled general circulation models (CGCMs); and to relate model differences to mean systematic error. The analysis is performed with long control simulations from ten CGCMs, with lengths ranging between 500 and 3600 years. In most models the variations of sea surface temperature (SST) averaged over North Atlantic show considerable power on multidecadal time scales, but with different periodicity. The SST variations are largest in the mid-latitude region, consistent with the short instrumental record. Despite large differences in model configurations, we find quite some consistency among the models in terms of processes. In eight of the ten models the mid-latitude SST variations are

J. Ba (✉) · M. Latif · W. Park · H. Ding
GEOMAR Helmholtz Centre for Ocean Research Kiel, Kiel, Germany
e-mail: jba@geomar.de

N. S. Keenlyside
Geophysical Institute and Bjerknes Centre, University of Bergen, Bergen, Norway

K. Lohmann
Max Planck Institute for Meteorology, Hamburg, Germany

J. Mignot
LOCEAN/IPSL, UPMC/CNRS/IRD/MNHN, University Pierre and Marie Curie, Paris, France

J. Mignot
Climate and Environmental Physics, Institute of Physics and Oeschger Center of Climate Research, University of Bern, Bern, Switzerland

M. Menary
Met Office Hadley Center, Exeter, UK

O. H. Otterå
Uni Research and the Bjerknes Centre, Bergen, Norway

B. Wouters
Royal Netherlands Meteorological Institute, De Bilt, The Netherlands

B. Wouters
School of Geographical Science, University of Bristol, Bristol, UK

B. Wouters
Department of Physics, University of Colorado at Boulder, Boulder, CO, USA

D. Salas y Melia
CNRM/GAME, Météo-France/CNRS, Toulouse, France

A. Oka
Atmosphere and Ocean Research Institute, University of Tokyo, Tokyo, Japan

A. Bellucci
Centro Euro-Mediterraneo per i Cambiamenti Climatici, CCMC, Bologna, Italy

E. Volodin
Institute of Numerical Mathematics RAS, INMRAS, Moscow, Russia

significantly correlated with fluctuations in the Atlantic meridional overturning circulation (AMOC), suggesting a link to northward heat transport changes. Consistent with this link, the three models with the weakest AMOC have the largest cold SST bias in the North Atlantic. There is no linear relationship on decadal timescales between AMOC and North Atlantic Oscillation in the models. Analysis of the key elements of the D93 mechanisms revealed the following: Most models present strong evidence that high-latitude winter mixing precede AMOC changes. However, the regions of wintertime convection differ among models. In most models salinity-induced density anomalies in the convective region tend to lead AMOC, while temperature-induced density anomalies lead AMOC only in one model. However, analysis shows that salinity may play an overly important role in most models, because of cold temperature biases in their relevant convective regions. In most models subpolar gyre variations tend to lead AMOC changes, and this relation is strong in more than half of the models.

Keywords Atlantic multidecadal variability (AMV) · Atlantic meridional overturning circulation (AMOC) · North Atlantic Oscillation (NAO) · Subpolar gyre (SPG)

1 Introduction

Atlantic multidecadal variability (AMV) with a time scale of 70–80 years in sea surface temperature (SST) has been found in a number of studies (Bjerknes 1964; Delworth and Mann 2000; Deser and Blackmon 1993; Knight et al. 2005; Kushnir 1994; Mann et al. 1998; Schlesinger and Ramankutty 1994). AMV is linked to Western African, American and European climate (Sutton and Hodson 2005; Knight et al. 2006; Enfield et al. 2001; Semenov et al. 2010; Zhang and Delworth 2006; Zhang et al. 2007). A number of studies have proposed mechanisms related to AMV, mainly based on results from climate models (Delworth et al. 1993; Delworth and Greatbatch 2000; Griffies and Tziperman 1995; Timmermann et al. 1998; Jungclaus et al. 2005).

Many model studies suggest the Atlantic meridional overturning circulation (AMOC) drives AMV in upper ocean temperature, because of its northward heat transport (Delworth et al. 1993; Timmermann et al. 1998; Jungclaus et al. 2005). In contrast, a few studies have suggested variations in external radiative (e.g., aerosol) forcing may have driven the observed AMV in SST (Booth et al. 2012). However, these studies are not able to fully explain observed variations in ocean heat content (Zhang et al. 2013), which were probably driven largely by ocean dynamics (Yeager et al. 2012; Gulev et al. 2013). It is currently not possible to confirm the oceanic origin of AMV from observations, as continuous measurements of AMOC have only become available since 2004, and only at 26.5°N (Cunningham et al. 2007). Because of the lack of adequate data on multidecadal time scale, ocean reanalysis has been used to assess past AMOC variations. However, there is little agreement among various ocean reanalyses. In particular, Keenlyside and Ba (2010) showed a wide spread in the strength and phase of the AMOC variations at 30°N among five systems from the EU ENSEMBLES project. Further north there are some agreements in terms of phase, but not strength (Pohlmann et al. 2013).

The strength of the AMOC is intimately tied to the three dimensional ocean density structures (Cunningham et al. 2007; Kanzow et al. 2007; Marotzke 1997; Hawkins and Sutton 2007). Observational and model studies also suggest a link among subpolar ocean wintertime convection, deep-water formation, and AMOC strength (Curry et al. 1998; Dickson et al. 1996; Marshall and Schott 1999; Delworth et al. 1993; Delworth and Greatbatch 2000; Timmermann et al. 1998; Jungclaus et al. 2005). The wintertime convection in the North Atlantic is observed in the Labrador Sea, Irminger Sea, and Nordic Seas (Dickson et al. 1996; Curry et al. 1998; Bacon et al. 2003; Pickart et al. 2003; Marshall and Schott 1999). However, the causes of convective variability are not fully understood. Hatun et al. (2005) suggested that as high-latitude sea surface temperatures are close to the freezing point in winter, density change is mainly determined by salinity, while Marshall and Schott (1999) indicated that high-latitude oceanic convection is caused by heat loss associated with atmospheric variability. In the latter case, oceanic changes can modulate the strength of convection by impacting the stability of the upper ocean.

Despite some model agreement on some processes, there remain significant differences in the mechanisms for simulated AMV among models. Delworth et al. (1993) placed importance on the interaction of the subpolar gyre (SPG) and AMOC, with anomalous salt advection to the sinking regions modulating the intensity of deep convection. While others found the AMOC to be modulated by freshwater export from the Arctic (Jungclaus et al. 2005) and subtropics (Vellinga and Wu 2004) into the sinking regions. Delworth and Greatbatch (2000) and Griffies and Tziperman (1995) suggested that the origin of the low-frequency time scales is from atmospheric stochastic forcing. However, Timmermann et al. (1998) propose a coupled positive feedback that amplifies oceanic variations.

Therefore, model intercomparison is important and necessary to better understand the reasons for model difference and to improve their representation of AMV. There have been a few multi-model comparisons related to AMV (Medhaug and Furevik 2011; Ting et al. 2011; Menary et al. 2012; Marini and Frankignoul 2013; Kavvada et al. 2013; Zhang and Wang 2013). Medhaug and Furevik (2011) analysed 24

coupled general circulation models (CGCMs) from coupled model intercomparison project phase 3 (CMIP3) database used for the intergovernmental panel on climate change (IPCC) fourth assessment report (AR4). They suggested the CGCMs could reproduce the observed warm and cold episodes during the twentieth century, and most models show a realistic structure in the overturning circulation. However, the CGCMs were forced by observed greenhouse gas concentration and direct effect of sulphate aerosols and natural forcing (volcanic aerosols and solar variability) from 1850 to 2000; and recent studies suggest these may be important drivers of North Atlantic SST changes in the historical period (Otterå et al. 2010; Booth et al. 2012).

Ting et al. (2011) indicated the strong relation between AMV and precipitation, and the clear physical mechanism for linkage in terms of meridional shifts of the Atlantic intertropical convergence zone (ITCZ) for the twentieth, twenty first centuries and preindustrial eras with 23 CGCMs. They focus on the AMV's climate impacts, such as Sahel rainfall. Menary et al. (2012) test the proposed mechanism in Vellinga and Wu (2004) with extended control simulations of three climate models. However, they only focus on the centennial variability. Here we present a multi-model comparison of unforced, internally generated AMV. Ten CGCMs have been used to investigate to what extent the climate models simulate observed AMV, and the similarities and differences among them.

Delworth et al. (1993) (hereafter D93) is an early work on simulated AMV mechanism that many studies compare to (Delworth and Greatbatch 2000; Timmermann et al. 1998; Vellinga and Wu 2004; Ba et al. 2013). Therefore, here a multi-model comparison is made to test the sensitivity of this mechanism to model formulation and the mean state. In particular, we investigate the ocean wintertime convection in different models and its relationship with AMOC, the temperature and salinity contributions to density anomalies in the convection regions that tend to precede the AMOC changes, and the relationship between the SPG and AMOC. We investigate also the relation between AMOC and SST, and the role of the North Atlantic Oscillation (NAO) in driving AMOC decadal variability.

The paper is organized as follows. Section 2 describes the ten CGCMs used in this study. Section 3 indicates the similarity of simulated AMV in these CGCMs to observations. Section 4 investigates the robustness of the mechanism proposed by D93 across the CGCMs. Summary and discussion follow in Sect. 5.

2 Model data

This study is based on ten coupled long control simulations, in which six models are contributed by the EU project THOR (Thermohaline Overturning—at risk?): the Bergen Climate Model (BCM) (Otterå et al. 2009), the Max Planck Institute for Meteorology Earth System Model (MPI-ESM-CR) (Jungclaus et al. 2010), the EC-EARTH (Hazeleger et al. 2012), the Institute Pierre Simon Laplace (IPSL-CM4) (Marti et al. 2010), the Kiel Climate Model (KCM) (Park et al. 2009; Park and Latif 2010) and the Hadley Center Climate Model (HadCM3) (Gordon et al. 2000; Pope et al. 2000). The other four models are the Centre National de Recherches Météorologiques Coupled Model (CNRM-CM3) (Guemas and Salas-Mélia 2008; Voldoire et al. 2013), the Centro Euro-Mediterraneo per i Cambiamenti Climatici (CMCC) (Bellucci et al. 2008), the Model for Interdisciplinary Research on Climate (MIROC) (K-1 model developers 2004; Oka et al. 2006) and the Institute of Numerical Mathematics Climate Model (INM-CM4) (Volodin et al. 2010). Key model details are listed in Table 1.

Table 1 List of unforced long control simulations with 10 CGCMs

Model	length (year)	Horizontal grid (Atm)	Horizontal grid (Ocn) (nominal)
BCM	700	T42	2.4°
MPI-ESM-CR	3000	T31	3°[a]
EC-EARTH	600	T159	1°
IPSL-CM4	1150	2.5° × 3.75°	2°
KCM	1000	T31	2°
HadCM3	1500	2.5° × 3.25°	1.25° × 1.25°
CNRM-CM3	1000	T42	2°
CMCC	759	T31	2°
MIROC	3600	T42	1.4° × 0.56°
INM-CM4	500	2° × 1.5°	1° × 0.5°

[a] Northern pole located over southern Greenland, convergence of mesh-size towards the poles translates into a grid spacing of 30–200 km in the North Atlantic

From the model output, all the indices are detrended. In correlation (regression) analysis among various indices and spatial fields, we filter the indices with an 11-year running mean to isolate the multidecadal signal. Significance tests applied account for the resulting reduced number of degrees of freedom.

3 Multi-model comparison of simulated North Atlantic multidecadal variability

Multidecadal variability is observed over the North Atlantic with a 70–80 year time scale, as illustrated by the AMV index (Fig. 1a; Knight et al. 2005; Enfield et al. 2001). The AMV index is defined as linearly detrended average SST over the North Atlantic (0°–60°N, 7.5°–75°W) (Sutton and Hodson 2005). The regression

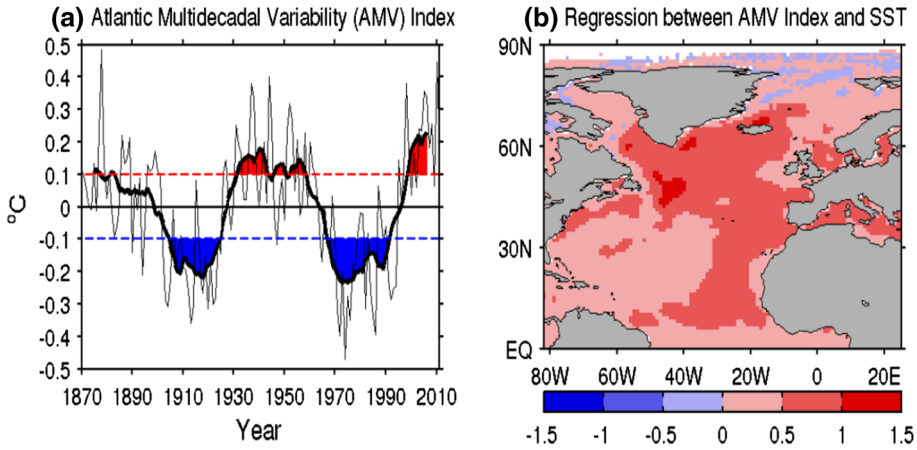

Fig. 1 **a** Observed Atlantic multidecadal variability (AMV) Index defined as linearly detrended North Atlantic (0–60°N) average sea surface temperature (SST). **b** The spatial pattern of observed SST variation over North Atlantic associated with the observed AMV Index by regressing the detrended SST on the normalized AMV index

Table 2 Mean SST averaged over the North Atlantic (0°–60°N, 7.5°–75°W) and the standard deviation of the AMV indices in observation and ten CGCMs

Observation/model	Mean (°C)	Standard deviation (°C)
Observation	21.08	0.26
BCM	18.34	0.12
MPI-ESM-CR	20.96	0.17
EC-EARTH	19.90	0.14
IPSL-CM4	19.31	0.21
KCM	18.60	0.18
HadCM3	20.48	0.21
CNRM-CM3	19.93	0.20
CMCC	19.61	0.14
MIROC	19.14	0.15
INM-CM4	18.78	0.36

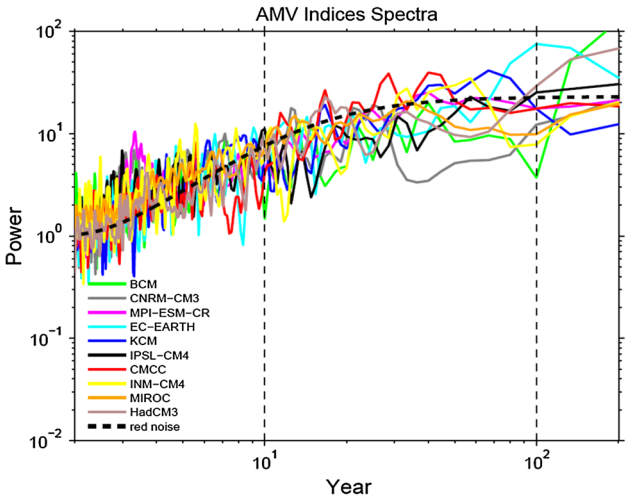

Fig. 2 The spectra of detrended AMV Indices in ten coupled general circulation models (CGCMs). The AR1 red noise fit is the mean of the AR1 red noise fits from ten models. Due to the varying autocorrelation for the models, the individual red-noise spectra are not shown

coefficients between the AMV index and SST are positive almost over the entire North Atlantic (Fig. 1b, Sutton and Hodson 2005). The region with largest positive regression is located in the mid-latitude (30°N–60°N) and eastern tropical North Atlantic, while the weaker regression values are in the western tropical and subtropical North Atlantic.

The simulated AMV indices in the ten models are calculated using the same definition as for observations. In all models, SST averaged over the North Atlantic (for the same region as the index) is colder than observed (Table 2). Except for INMCM4, the models simulate weaker AMV than observed during the instrumental period (Table 2). These differences could result from the external forcing that is fixed to preindustrial conditions in the most control simulations.

The corresponding power spectra of the simulated AMV indices show a wide range of variability, but exhibit a similar red noise character (Fig. 2). Most AMV indices show power on multi-decadal time scales, but with different periodicity. The spatial patterns of SST variation associated with the AMV index in the ten models are illustrated in Fig. 3. The regression patterns show similarities with the observations in most models, with the largest loadings in the mid-latitude region and weaker regression in the western tropical and subtropical North Atlantic. However, the regression values are higher than in observations. Except for CNRM-CM3, KCM and IPSL-CM4, the regressions in the eastern tropical and subtropical region are weaker than mid-latitude region. The INM-CM4 has the weakest regression over the North Atlantic. HadCM3 shows the strongest negative regression over the Arctic region and MIROC shows the strongest negative regression values in the Greenland-Iceland-Norwegian (GIN) Sea region. In addition to model error, differences in patterns could also be related to observational uncertainties as well as the absence of time varying external forcing in our simulations.

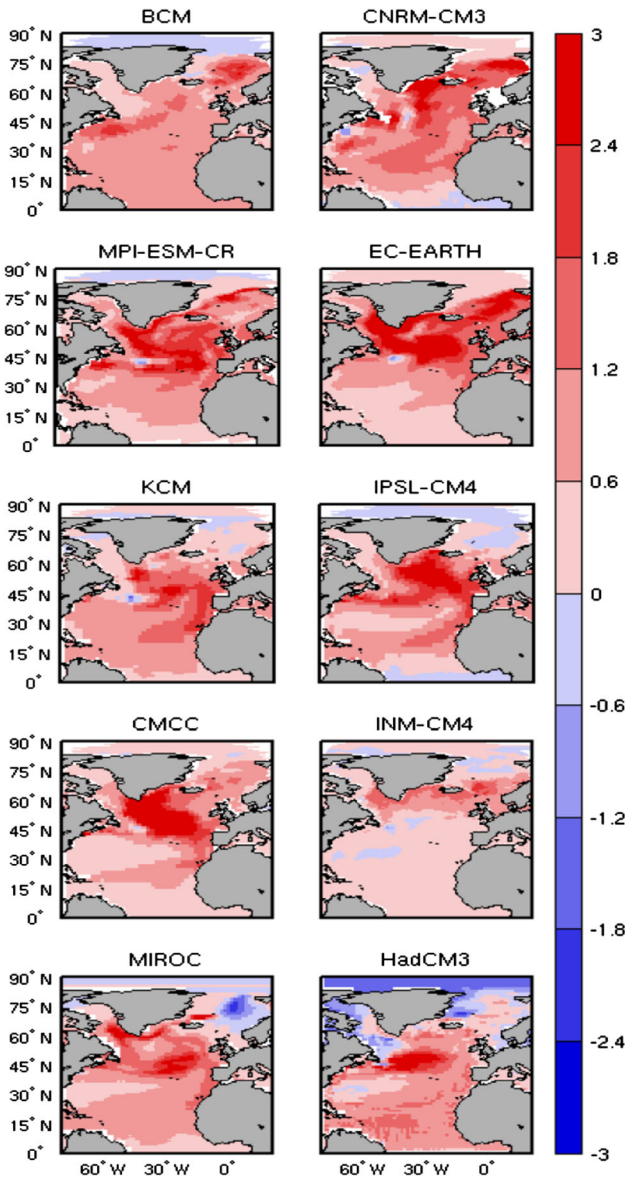

Fig. 3 The spatial patterns of SST variations over North Atlantic associated with the AMV indices in ten CGCMs. The regressions are calculated by detrended SSTs and AMV indices in ten models

Atlantic multidecadal variability (AMV) is thought to be strongly linked to fluctuations in the AMOC, through associated variations in the northward heat transport (Hall and Bryden 1982; Delworth et al. 1993; Timmermann et al. 1998; Delworth and Mann 2000; Latif et al. 2004; Jungclaus et al. 2005; Gastineau and Frankignoul 2012). This is consistent with the larger mid-latitude loadings in the SST variability pattern related to AMV (Fig. 3). Figure 4 shows the time mean North Atlantic meridional overturning stream functions for the ten models. In each model the stream function has a maximum located from 30°N to 50°N. Compared to the mean value of the observed AMOC (17.4Sv) from the RAPID array at 26.5°N (Cunningham et al. 2007), the AMOC strength in BCM, CNRM-CM3, and MIROC at the same latitude are stronger. However, KCM, IPSL-CM4 and CMCC have relatively weak transport. The AMOC strength in MPI-ESM-CR, EC-EARTH and HadCM3 are closest to the observed value. We note that the INM-CM4 AMOC weakens by around 2.5Sv (not shown) over the course of the simulation, which is limited in length by computational resources; this drift may contribute to the weaker AMV pattern (Fig. 3). The large spread in AMOC strength among models remains to be fully explained. Further, the large uncertainty in the observational estimate from RAPID should be also considered in this context.

In many models, AMOC anomalies propagate southward with a time scale of several years from the subpolar to the subtropical region, because of the contribution of the slower interior transport in this region (Zhang 2010). Cross-correlation of the AMOC indices at 45°N with AMOC indices at lower latitudes indicates that these ten models also behave similarly (Fig. 5), where the AMOC indices are defined as the maximum Atlantic meridional overturning stream function at the different latitudes. In all models AMOC at 45°N leads AMOC at 30°N by a few years with a high correlation. Unless otherwise indicated, in further analysis the AMOC indices are defined as the maximum Atlantic meridional overturning stream function at 30°N, because the strength of the overturning stream function at 30°N is generally much higher than at other latitudes.

To assess the role of the AMOC in AMV the lead-lag relationship between the AMV and AMOC indices is computed (Fig. 6a). In five models (EC-EARTH, KCM, IPSL-CM4, CMCC, HadCM3) AMOC and AMV indices variations are strongly related and almost in phase. EC-EARTH and CMCC show AMV leads AMOC by about 1–2 years, while KCM, IPSL-CM4 and HadCM3 show AMV lags AMOC by about 1–5 years. Consistent with Fig. 5, variations in AMOC at 45°N lead AMV by several years in all models, except for INM-CM4; the relation is also overall stronger (not shown). The AMOC index spectra are shown in Fig. 6b. The AMOC indices show power on multi-decadal time scales, but with different periodicity. While the spectra have an overall red character, there are notable differences to the spectra of an AR-1 process, as expected (Mecking et al. 2013). Cross-spectral analyses for the five models with the strongest AMOC and AMV relation confirm that this relationship occurs on multidecadal timescales (not shown). These relationships between SST and AMOC simulated in models differ over the North Atlantic. Figure 6c shows the cross-correlation between AMV indices and the averaged SST over the tropical and subtropical region in the North Atlantic. Figure 6d illustrates the relationship in the mid-latitude North Atlantic. It indicates that the significant relationship between AMV and AMOC is mainly located in the mid-

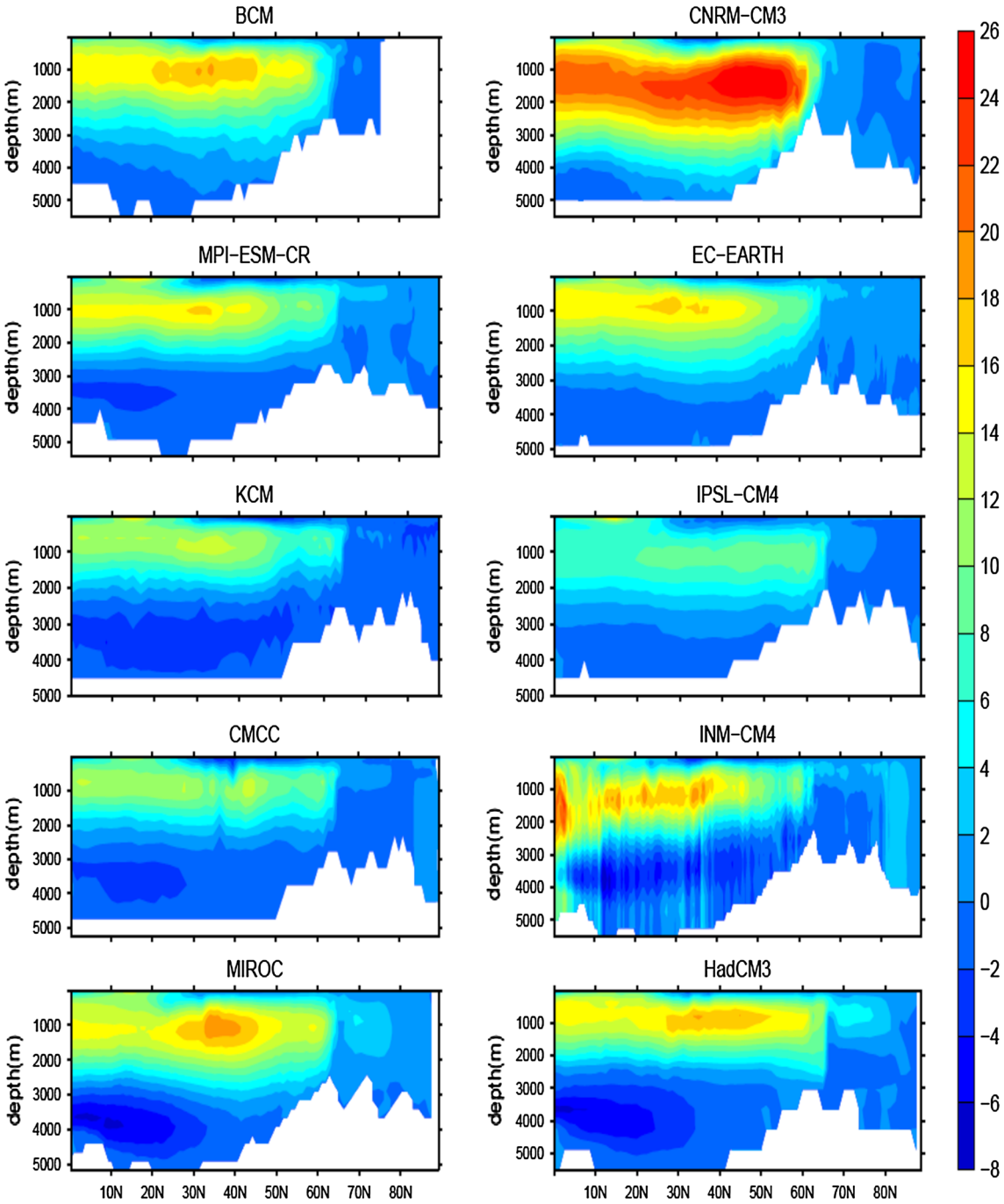

Fig. 4 The mean state of Atlantic meridional overturning circulation (AMOC) stream function in ten CGCMs

latitude North Atlantic, which is consistent with the patterns shown in Fig. 3.

It has been suggested that AMOC fluctuations that affect the North Atlantic SST variations are linked to the NAO (Visbeck et al. 1998; Eden and Jung 2001). Latif et al. (2006) and Latif and Keenlyside (2011) showed that low-frequency variability of an SST based AMOC index lags the NAO by about one decade. However, this relationship between the AMOC and NAO is not clear in these ten models (Fig. 7). The power spectra of the model NAO indices show that they are essentially consistent with white noise (Fig. 7a). The relationships between AMOC indices and NAO indices in the ten models are not significant (Fig. 7b). This is consistent with the analysis of EC-EARTH from Wouters et al. (2012); and the analysis of the BCM by Medhaug et al. (2012), which identify a link between AMOC and the NAO with low explained variance ($\sim$11 %). However, the atmosphere's role needs further exploration.

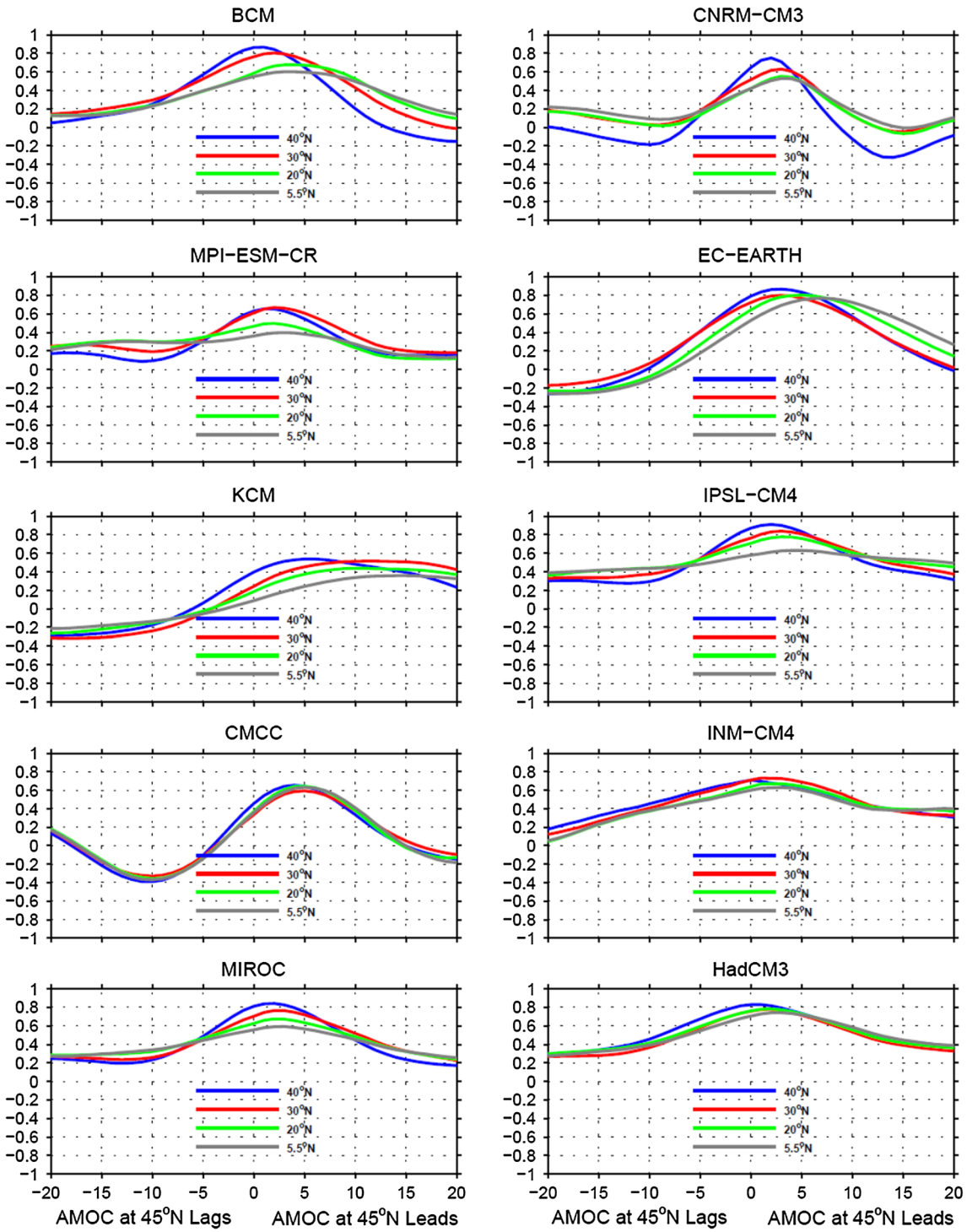

Fig. 5 The cross-correlation between AMOC indices at 45°N and AMOC indices at 40°N, 30°N, 20°N, 5.5°N, respectively in ten CGCMs

4 Multi-model mechanism assessments to key aspect of D93

D93 is one of the earliest studies to investigate the mechanism behind AMV, and is often mentioned and compared to in other works (Delworth and Greatbatch 2000; Timmermann et al. 1998; Vellinga and Wu 2004; Ba et al. 2013). In D93 AMOC variations on multidecadal timescales are driven by changes of North Atlantic high-latitude density, associated with wintertime oceanic convection. The key aspects of D93 are compared here among our ten CGCMs.

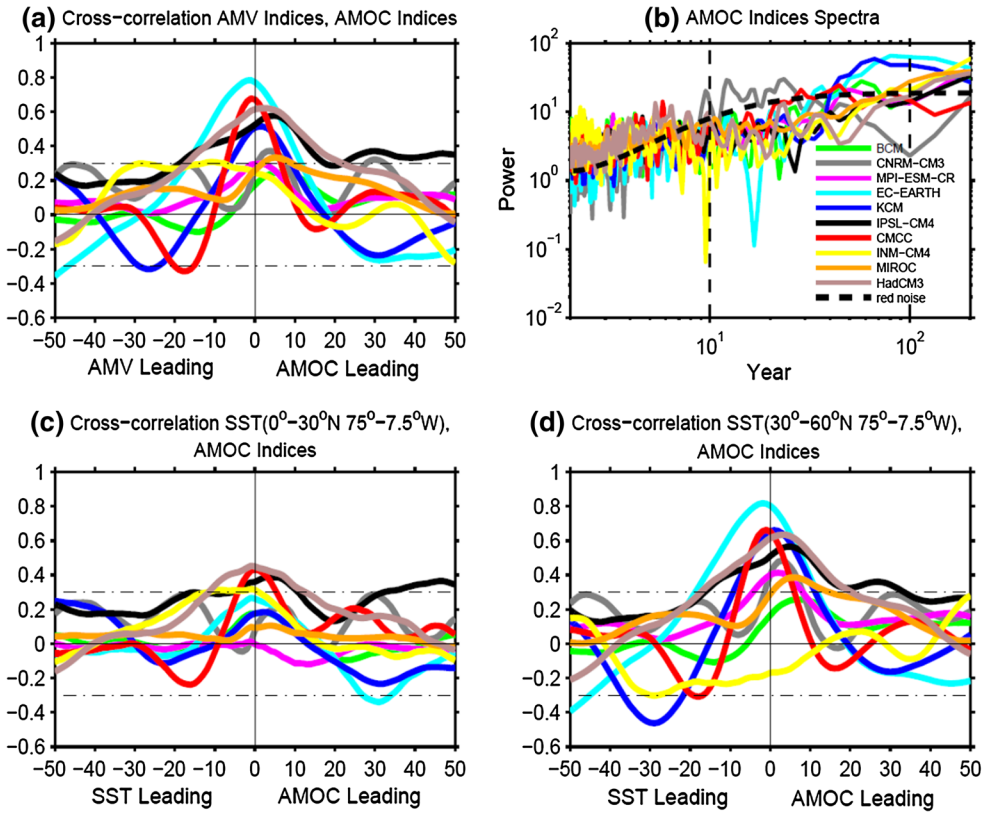

Fig. 6 **a** Cross-correlations among AMV indices and AMOC indices at 30°N in ten CGCMs. **b** Power spectra of AMOC indices at 30°N. The AR1 red noise fit is the mean of AR1 red noise fits from ten models. **c** Cross-correlation between averaged SST (0°–30°N) in North Atlantic and AMOC indices at 30°N. **d** Cross-correlation between averaged SST (30°–60°N) in North Atlantic and AMOC indices at 30°N. For the correlations an 11-year running mean is applied and the 95 % confidence level is around 0.3 (*black dotted line*) in each model

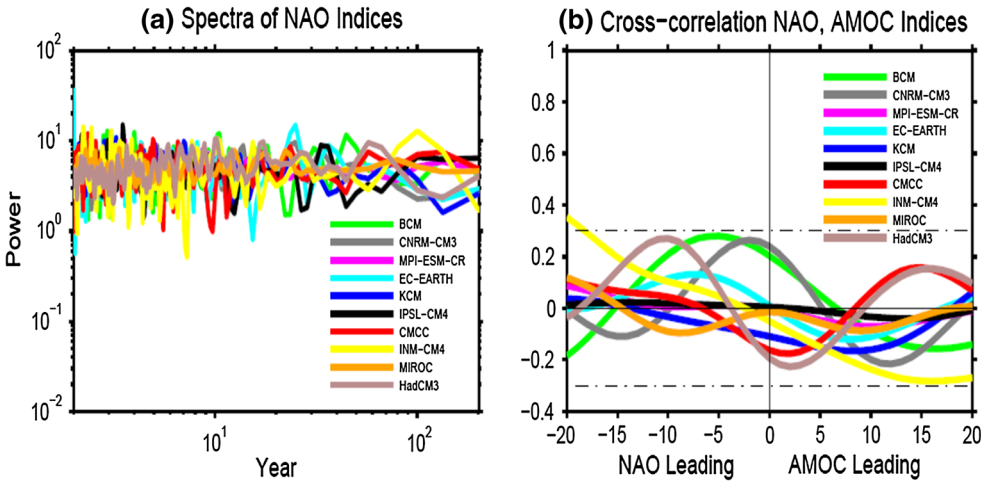

Fig. 7 **a** Power spectra of North Atlantic Oscillation (NAO) indices in ten CGCMs. **b** Cross-correlation among AMOC indices at 30°N and NAO indices. For the correlations an 11-year running mean is applied and the 95 % confidence level is around 0.3 (*black dotted line*) in each model

We analyze the relationship between the AMOC and specific convection regions in the different models. This is a slightly different approach to D93, who considered the Atlantic region from 52° to 72°N as the sinking region for AMOC, and did not specify the individual convection regions. The relative importance of different convection sites across the models may have implications for the model's susceptibility to different mechanisms of internal and externally-forced variability, a feature which would have been masked by choosing a broader North Atlantic convection region.

Wintertime mixed-layer depth (MLD) is used here as a measure of oceanic convection and deep water formation. Surface buoyancy fluxes drive deep water formation by

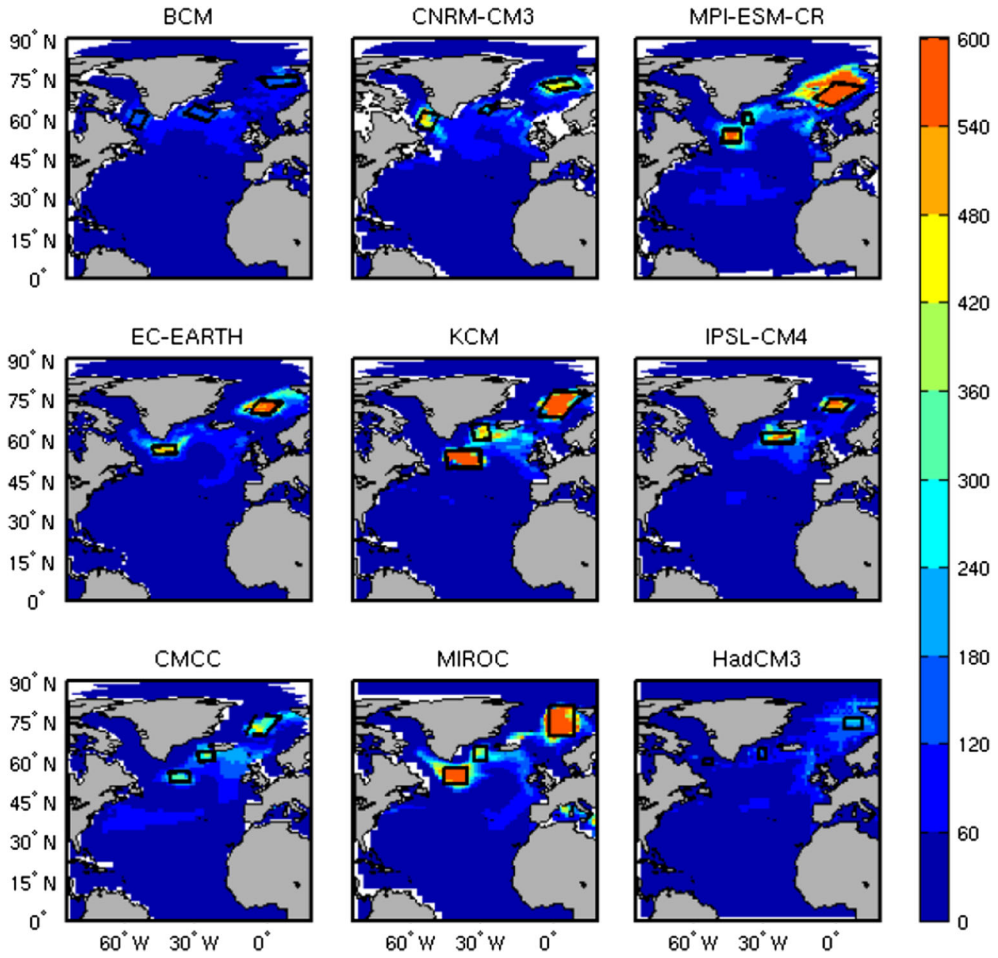

Fig. 8 The standard deviation of winter mixed layer depth (MLD) in nine CGCMs (data from INM-CM4 is not available). The region with the largest mean state is same with the largest standard deviation. The convection regions for the further analysis are highlighted by black boxes in every model respectively

causing both large-scale sinking and convective overturning (Isachsen et al. 2007; Lazier et al. 2002). Although convection cannot directly drive meridional overturning circulation changes, as it only involves vertical mass exchange, observations and models suggest a close relation among MLD, deep water formation, and changes in overturning strength (Eden and Willebrand 2001; Curry et al. 1998; Dickson et al. 1996). Thus, MLD is often used as an indicator for oceanic convection in connection with AMOC changes (Delworth et al. 1993; Jungclaus et al. 2005; Wouters et al. 2012; Ba et al. 2013). Nevertheless, MLD in BCM is not an ideal proxy for oceanic convection, because of the mixing scheme implemented in this isopycnal model (Medhaug et al. 2012); we only use it here for consistency. In the nine models (INM-CM4 MLD data is not available) the regions with the largest standard deviation in wintertime mixed layer depth correspond to the regions with the deepest mean MLD, and are used to determine the regions of wintertime deep convection. The standard deviation is used here to define the convective regions since we focus on the variability.

The regions of wintertime deep oceanic convection differ among the models (Fig. 8): there are three models with Labrador Sea convection (BCM, CNRM-CM3 and HadCM3); eight with Irminger Sea convection (BCM, CNRM-CM3, MPI-ESM-CR, KCM, IPSL-CM4 (eastern Irminger Sea), CMCC, MIROC and HadCM3); five with South Greenland Sea convection (MPI-ESM-CR, EC-EARTH, KCM, CMCC and MIROC); and all nine with GIN Sea convection. Wintertime convection in BCM and HadCM3 are much shallower than in the other models. South Greenland Sea convection was not observed during the instrumental record. However, its presence in models is likely related to model bias that is discussed later.

Figure 9 shows the cross-correlation between convection indices (defined as the averaged MLD in the boxes depicted in Fig. 8) and AMOC indices at 30°N in the nine models. Labrador Sea convection indices are not

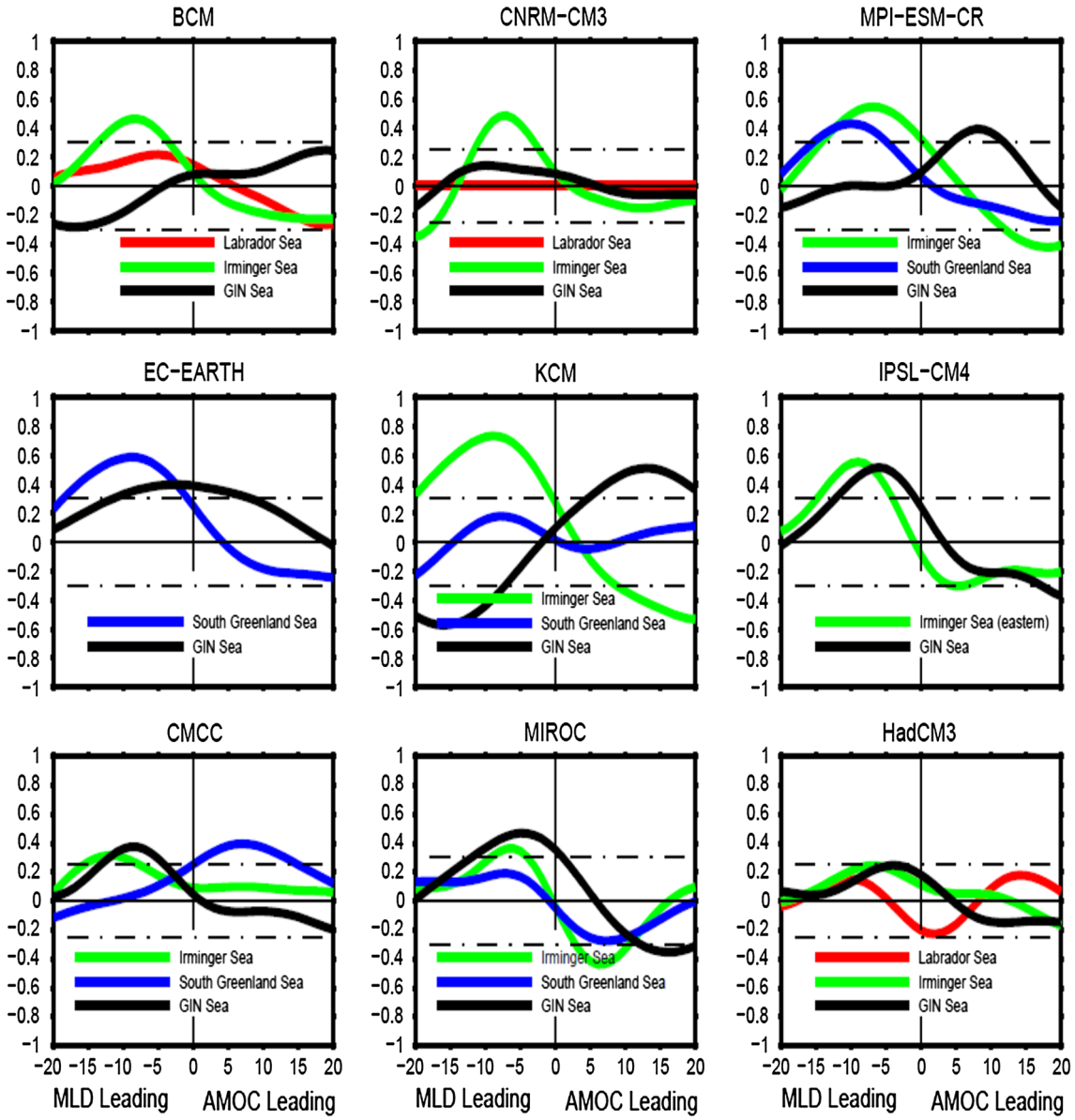

Fig. 9 The cross-correlations between convections and AMOC indices at 30°N in nine CGCMs (data from INM-CM4 is not available). Labrador Sea in *red line*; Irminger Sea in *green line*; South Greenland Sea in *blue line*; GIN Sea in *black line*. For the correlations an 11-year running mean is applied and the 95 % confidence level is around 0.3 (*black dotted line*) in each model

significantly related with variations in the AMOC in the three models with convection in this region. However, Medhaug et al. (2012) used a different convection definition (not MLD) and find the relationship between Labrador Sea and AMOC in BCM, while Guemas and Salas-Mélia (2008) showed the AMOC index defined at 50°–60°N lags Labrador Sea convection by 1 year in CNRM-CM3. Irminger Sea convection is seen in eight models (apart from EC-EARTH) and tends to precede the AMOC, most significantly by about 10 years in five models (BCM, CNRM-CM3, MPI-ESM-CR, KCM and IPSL-CM4). South Greenland Sea convection significantly leads the AMOC only in EC-EARTH, consistent with Wouters et al. (2012). The GIN Sea convection leads the AMOC index in CMCC and MIROC. Thus, in eight models (BCM, CNRM-CM3, MPI-ESM-CR, EC-EARTH, KCM, IPSL-CM4, CMCC and MIROC) high-latitude density anomalies due to wintertime convection significantly precede decadal AMOC changes, but uncertainty exists in the importance of various convection sites.

In D93 the density anomalies in the sinking region that drive AMOC changes are dominated by anomalous salinity. Here we also investigate the relationship between the AMOC and temperature and salinity contributions to

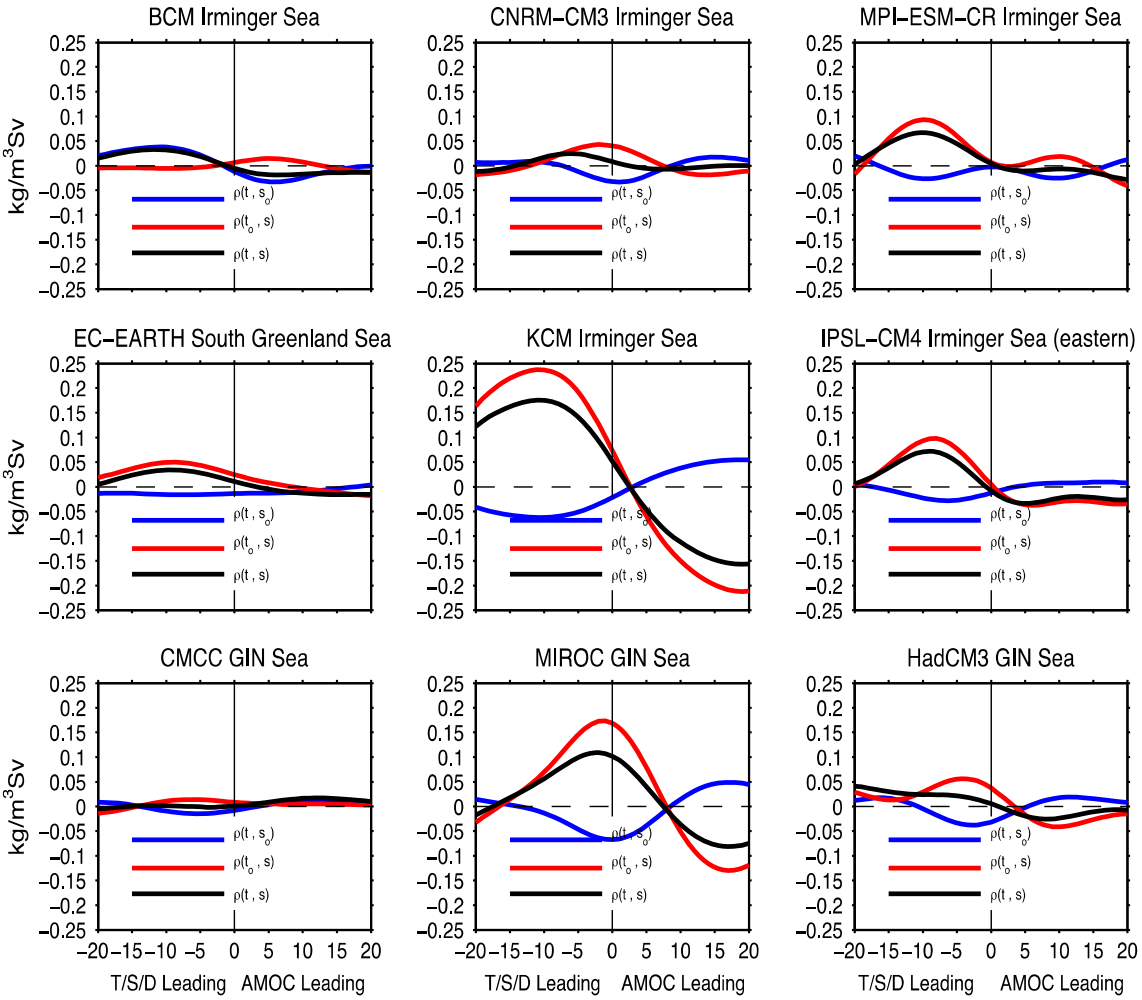

Fig. 10 The cross-regressions of the AMOC indices at 30°N with density variation (*black*) and corresponding contribution of temperature (*blue*), salinity (*red*) to density in convection regions in nine CGCMs. In each model, we only show these relationships in the sinking regions where increased MLD most highly and significantly leads AMOC changes. For the regression an 11-year running mean is applied

density in the sinking regions in different models (Fig. 10). In each model, we only show these relationships in the sinking regions where increased MLD most significantly leads AMOC changes. Among the eight models (BCM, CNRM-CM3, MPI-ESM-CR, EC-EARTH, KCM, IPSL-CM4, CMCC and MIROC) in which wintertime convection tends to strongly lead the AMOC, salinity anomalies play the most important role in seven models (Irminger Sea in CNRM-CM3, MPI-ESM-CR, KCM and IPSL-CM4; South Greenland Sea in EC-EARTH; GIN Sea in CMCC and MIROC). KCM shows the strongest salinity-induced density anomaly in wintertime Irminger Sea convection that drives AMOC fluctuations. BCM is the only model in which temperature variations control the increase in density prior to maximum AMOC. In the other seven models temperature appears to counter balance the salinity driven density anomalies.

D93 indicate that SPG variations control the transport of anomalous salinity to the sinking region. The SPG index is defined as the absolute maximum of the barotropic streamfunction in the subpolar region. The relationship between the SPG and AMOC is shown in Fig. 11 for only nine models, because the barotropic streamfunction data for CMCC is not available. SPG leads AMOC significantly in eight models and strongly in five models (BCM, CNRM-CM3, EC-EARTH, KCM, IPSL-CM4). SPG variations are not the only possible mechanism controlling salinity in the sinking regions. Other possibilities for example include advection of salinity from high-latitudes (Jungclaus et al. 2005) or mean advection of anomalous salinity from the low-latitudes (Vellinga and Wu 2004; Menary et al. 2012). Analyzing the origin of the salinity-induced density anomalies that appear in the sinking regions is beyond the scope of this study.

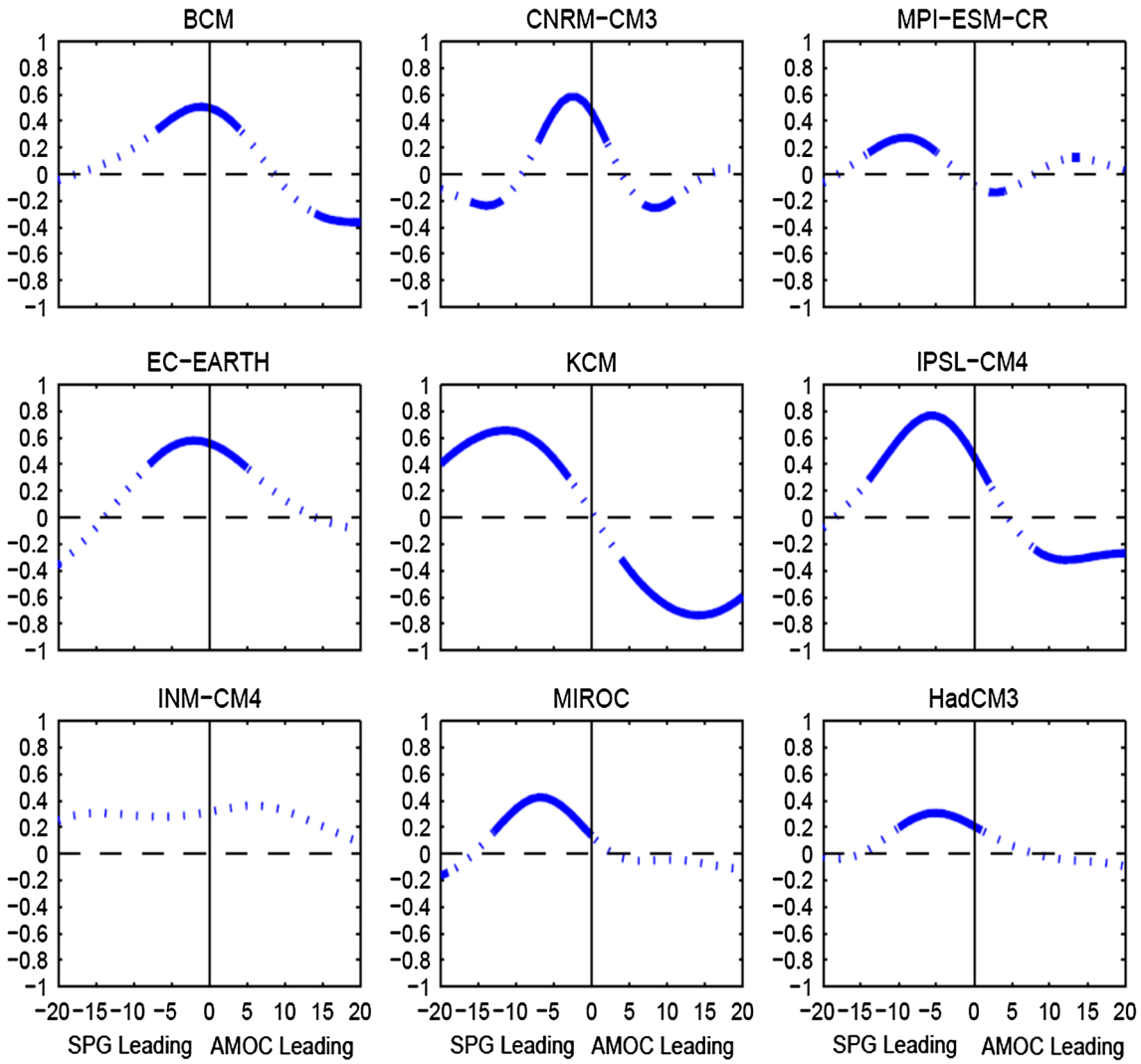

Fig. 11 The cross-correlations between subpolar gyre (SPG) and AMOC indices at 30°N in nine CGCMs (data from CMCC is not available). The *solid* parts of the *curves* are significant at the 95 % level

5 Summary and discussion

Lack of instrumental data in length and spatial coverage prevent us from understanding AMV. Therefore CGCMs provide an alternative and useful tool to investigate the mechanisms of internal variability on the decadal to multidecadal time scale. However, the mechanisms differ from model to model. Thus a multi-model comparison of AMV is performed here to understand the similarity to observations in unforced long control simulations by ten CGCMs and check the robustness of the mechanism proposed by D93 with respect to model configuration. AMV indices in most models show considerable power on multidecadal time scales, but with different periodicity. The SST patterns related to AMV in the models are largely similar to the observed pattern. Thus, given the limited instrumental record, it is difficult to conclude any of the ten models are inconsistent with observations.

The key findings of this paper are summarized in Fig. 12. In observations and models, the SST pattern related to AMV shows largest loadings in the mid-latitude North Atlantic region. This is consistent with the significant relationship between mid-latitude SST and AMOC at 30°N found in most (8/10) models. When considering the AMV index (i.e., SST over the 0–60°N North Atlantic), only the five models with pronounced multi-decadal variability show a clear relation between AMOC and AMV. The relationship between the AMOC and NAO is not clear in any of the models. This is in contrast to evidence from observational studies and a few modeling studies (Eden and Jung 2001; Delworth and Greatbatch 2000; Latif et al. 2006; Latif and Keenlyside 2011).

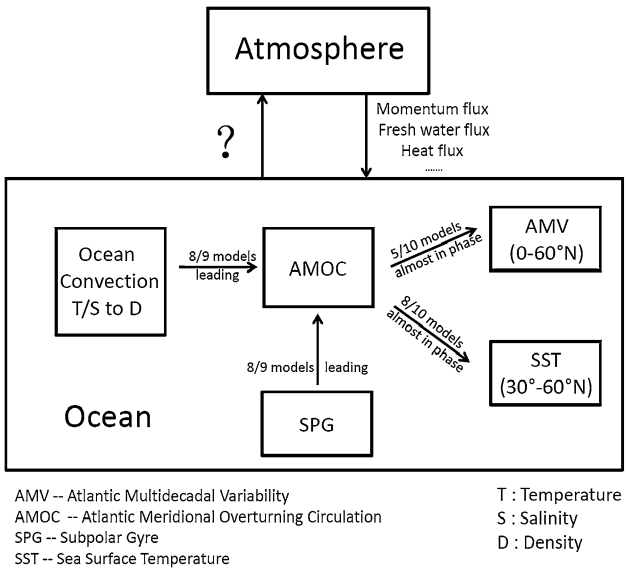

Fig. 12 The schematic for the summary of mechanism. The AMV is significantly correlated with AMOC in five out of ten models. The SST pattern related to AMV shows largest loadings in the mid-latitude Atlantic region, consistent with the significant relationship between mid-latitude SST and AMOC found in eight out of ten models. Eight out of nine models show the strong and significant link between wintertime convection and AMOC. Seven models show that the AMOC variation is driven by salinity-induced density anomalies in the convection region, while one model by temperature-induced density anomalies. And SPG leads AMOC significantly in eight out of nine models and strongly in five

Compared to the main mechanism of D93, despite the differences in model configuration, a certain degree of consistency is found among the models. In essentially all models (8/9) there is a deepening of the wintertime mixed layer depth in at least one of the deep convection sites 5–10 years prior to a strengthening AMOC. However, the sites and strength of this relation differ, suggesting the need for other indices for deep water formation. In most of these models (7/8) salinity variations control density changes in the convective regions where mixed layer deepening precedes AMOC strengthening. The SPG variations significantly lead AMOC changes in most models (8/9) and strongly in five models.

However, the models inevitably depict some differences. The reason for the disagreement among models in their representation of the different processes could be related to their simulated mean climate states, which differ from the observed (and each other). The model SST biases are shown in Fig. 13. Except for BCM and CNRM-CM3, the other models show a cold bias in the mid-latitude North Atlantic (Randall et al. 2007). In particular, three models (KCM, IPSL-CM4 and CMCC) have a colder bias than others, which might be because of their weak AMOC in North Atlantic (Fig. 4). However, the variance of the AMV index (Table 2) or its structure (Fig. 3) cannot be clearly related to the SST bias (Fig. 13).

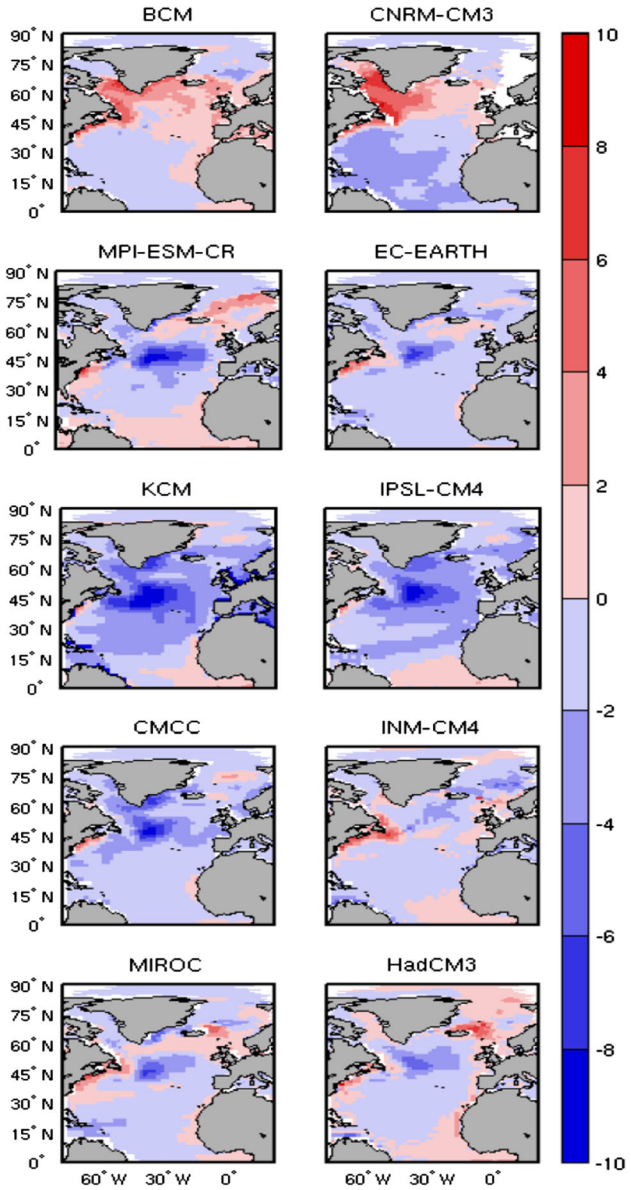

Fig. 13 The annual mean SST compared to observation from the Levitus data in ten CGCMs (model minus observation)

The cold conditions in the North Atlantic might enhance the role of salinity in AMV because in the colder regions salinity tends to dominate the density anomalies. This could be due to the thermal expansion coefficient of water at standard pressure which becomes quite small when the water temperature approaches the freezing point (Delworth et al. 1993) and the non-linearity of the equation of state for density; but an increase of sea ice also tends to strengthen the salinity impact. On the other hand, in the warmer regions thermal effects tend to dominate, so the warm bias over the subpolar region might be the reason why density anomalies in the sinking region result from temperature changes in BCM. In addition, warmer conditions decrease

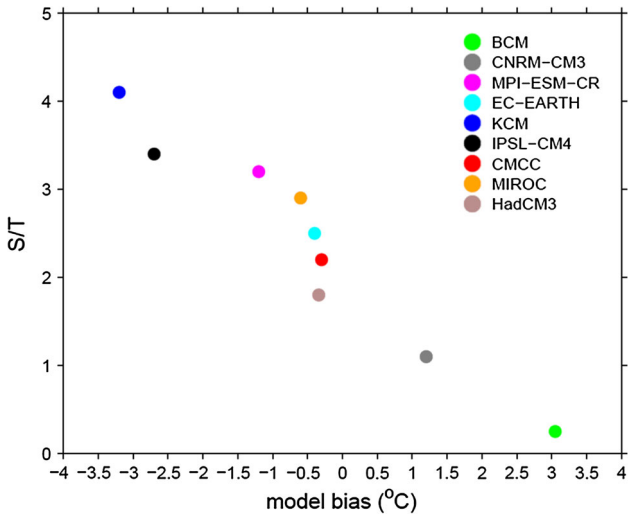

Fig. 14 The relationship between the mean temperature bias and ratio of salinity and temperature contributions to density changes in ten CGCMs. The temperature bias is defined as the difference to Levitus' climatology (model minus observation). The vertical axis shows the ratio of salinity-induced density anomalies to temperature-induced density anomalies. The salinity-induced density anomalies are computed with the simulated salinity anomalies and climatological temperature; and vice versa for temperature-induced density anomalies. All numbers were computed for the convection region which is related to AMOC variations in each model

the sea ice and subsequently weaken the salinity impact. Further analysis confirms a close relation between model temperature biases and the relative importance of salinity in density variability (Fig. 14). It shows a clear linear relationship between the temperature bias and the absolute ratio of the salinity-induced density anomaly to the temperature-induced density anomaly in the convection region of each model that are related to AMOC variations. The BCM and CNRM-CM3 have the lower value with the warm model bias, while other models have the large value with the cold bias. The result suggests that salinity variability is overly important in most models. Furthermore, the existence of South Greenland Sea convection in some models, which was not observed, also might be a result of model bias. Therefore, it is important to understand the impact of model biases on AMV and its predictability, and to identify strategies to bias correct forecasts in different models.

Acknowledgments We thank the Deutsche Forschungsgemeinshaft under the Emmy Noether programme (Grant KE 1471/2-1) supported JB and NK. Support from the European Community's 7th framework programme (FP7/2007–2013) under grant agreement No. GA212643 (THOR: Thermohaline circulation—at risk? 2008–2012), No. 266722 (SUMO) and PCIG10-GA-2011-304243 (STEPS); RACE project funded by German Federal Ministry for Education and Research; and the Centre for Climate Dynamics are acknowledged. Computing resources from GEOMAR and Rechenzentrum der Universität Kiel are greatly appreciated.

References

Ba J, Keenlyside NS, Park W, Latif M, Hawkins E, Ding H (2013) A mechanism for Atlantic multidecadal variability in the Kiel Climate Model. Clim Dyn 41:2133–2144. doi:10.1007/s00382-012-1633-4

Bacon S, Gould WJ, Jia Y (2003) Open-ocean convection in the Irminger Sea. Geophys Res Lett 30(C5):1246

Bellucci A, Gualdi S, Scoccimarro E, Navarra A (2008) NAO-ocean interactions in a coupled general circulation model. Clim Dyn 31:759–777. doi:10.1007/s00382-008-0408-4

Bjerknes J (1964) Atlantic air-sea interaction. Adv Geophys 10:1–82

Booth BBB, Dunstone NJ, Halloran PR, Andrews T, Bellouin N (2012) Aerosols implicated as a prime driver of twentieth-century North Atlantic climate variability. Nature 484:228–232. doi:10.1038/nature10946

Cunningham SA, Kanzow T, Rayner D, Baringer MO, Johns WE, Marotzke J, Longworth HR, Grant EM, Hirschi JJM, Beal LM, Meinen CS, Bryden HL (2007) Temporal variability of the Atlantic meridional overturning circulation at 26.5 degrees N. Science 317(5840):935–938. doi:10.1126/science.1141304

Curry RG, McCartney MS, Joyce TM (1998) Oceanic transport of subpolar climate signals to mid-depth subtropical waters. Nature 391:575–577

Delworth TL, Greatbatch RJ (2000) Multidecadalthermohaline circulation variability driven by atmospheric surface flux forcing. J Clim 13:1481–1495

Delworth TL, Mann ME (2000) Observed and simulated multidecadal variability in the Northern Hemisphere. Clim Dyn 16:661–676

Delworth TL, Manabe S, Stouffer RJ (1993) Interdecadal variations of the thermohaline circulation in a coupled ocean-atmosphere model. J Clim 6:1993–2011

Deser C, Blackmon ML (1993) Surface climate variations over the North-Atlantic Ocean during winter—1900–1989. J Clim 6:1743–1753

K-1 model developers (2004) In: Hasumi H, Emori S (Eds), Coupled GCM (MIROC) description, K-1. Technical report No. 1

Dickson R, Lazier J, Meincke J, Rhines P, Swift J (1996) Longterm coordinated changes in the convective activity of the North Atlantic. Prog Oceanogr 38:241–295

Eden C, Jung T (2001) North Atlantic interdecadal variability: oceanic response to the North Atlantic Oscillation (1865–1997). J Clim 14:676–691

Eden C, Willebrand J (2001) Mechanism of interannual to decadal variability of the North Atlantic circulation. J Clim 14:2266–2280

Enfield DB, Mestas-Nuñez AM, Trimble PJ (2001) The Atlantic Multidecadal Oscillation and its relation to rainfall and river flows in the continental U. S. Geophys Res Lett 28:2077–2080

Gastineau G, Frankignoul C (2012) Cold-season atmospheric response to the natural variability of the Atlantic meridional overturning circulation. Clim Dyn 39:37–57

Gordon C, Cooper C, Senior C, Banks H, Gregory J, Johns T, Mitchell J, Wood R (2000) The simulation of SST, sea ice extents and ocean heat transports in a version of the Hadley Centre coupled model without flux adjustments. Clim Dyn 16:147–168

Griffies SM, Tziperman E (1995) A linear thermohaline oscillator driven by stochastic atmospheric forcing. J Clim 8:2440–2453

Guemas V, Salas-Mélia D (2008) Simulation of the Atlantic meridional overturning circulation in an atmosphere–ocean global coupled model. Part I: a mechanism governing the variability of ocean convection in a preindustrial experiment. Clim Dyn 31(1):29–48

Gulev SK, Latif M, Keenlyside NS, Park W, Koltermann KP (2013) North Atlantic Ocean control on surface heat flux on multidecadal timescales. Nature. doi:10.1038/nature12268

Hall M, Bryden H (1982) Direct estimates and mechanisms of ocean heat transport. Deep Sea Res Part A 29:339–359

Hatun H, Sando AB, Drange H, Hansen B, Valdimarsson H (2005) Influence of the Atlantic subpolar gyre on the thermohaline circulation. Science 309:1841–1844

Hawkins E, Sutton R (2007) Variability of the Atlantic thermohaline circulation described by three-dimensional empirical orthogonal tunctions. Clim Dyn 29:745–762

Hazeleger W, Wang X, Stefanescu S, Severijns C, Bintanja R, Sterl A, Wyser K, Semmler T, Yang S, van den Hurk B, van Noije T, van der Linden E, van der Wiel K (2012) EC-Earth V2.2: description and validation of a new seamless earth system prediction model. Clim Dyn 39:2611–2629

Isachsen PE, Mauritzen C, Svendsen H (2007) Dense water formation in the Nordic Seas diagnosed from sea surface buoyancy fluxes. Deep Sea Res I 54:22–41

Jungclaus JH, Haak H, Latif M, Mikolajewicz U (2005) Arctic-North Atlantic interactions and multidecadal variability of the meridional overturning circulation. J Clim 18:4013–4031

Jungclaus JH et al (2010) Climate and carbon-cycle variability over the last millennium. Clim Past 6:723–737

Kanzow T, Cunningham SA, Rayner D, Hirschi JJM, Johns WE, Baringer MO, Bryden HL, Beal LM, Meinen CS, Marotzke J (2007) Observed flow compensation associated with the MOC at 26.5 degrees N in the Atlantic. Science 317(5840):938–941

Kavvada A, Ruiz-Barradas A, Nigam S (2013) AMO's structure and climate footprint in observations and IPCC AR5 climate simulations. Clim Dyn. doi:10.1007/s00382-013-1712-1

Keenlyside NS, Ba J (2010) Prospects for decadal climate prediction. Wiley Interdiscip Rev Clim Change 1(5): 627–635. ISSN 1757-7799

Knight JR, Allan RJ, Folland CK, Vellinga M, Mann ME (2005) A signature of persistent natural thermohaline circulation cycles in observed climate. Geophys Res Lett 32:L20708

Knight JR, Folland CK, Scaife AA (2006) Climate impacts of the Atlantic Multidecadal Oscillation. Geophys Res Lett 33:L17706

Kushnir Y (1994) Interdecadal variations in North Atlantic Sea surface temperature and associated atmospheric conditions. J Clim 7:141–157

Latif M, Keenlyside NS (2011) A perspective on decadal climate variability and predictability. Deep Sea Res 10:1016

Latif M et al (2004) Reconstructing, Monitoring, and Predicting Multidecadal-Scale changes in the North Atlantic thermohaline circulation with sea surface temperature. J Clim 17:1605–1614

Latif M, Collins M, Pohlmann H, Keenlyside N (2006) A review of predictability studies of Atlantic sector climate on decadal time scales. J Clim 19:5971–5987

Lazier J, Hendry R, Allyn Clarke, Yashayaev I, Rhines P (2002) Convection and restratification in the Labrador Sea, 1990–2000. Deep Sea Res I 49:1819–1835

Mann ME, Bradley RS, Hughes MK (1998) Global-scale temperature patterns and climate forcing over the past six centuries. Nature 392:779–787

Marini C and Frankignoul C (2013) An attempt to deconstruct the Atlantic Multidecadal Oscillation. Clim Dyn. doi:10.1007/s00382-013-1852-3

Marotzke J (1997) Boundary mixing and the dynamics of three-dimensional thermohalinecirculations. J Phys Oceanogr 27:1713–1728

Marshall J, Schott F (1999) Open-ocean convection: observations, theory, and models. Rev Geophys 37:1–64

Marti O et al (2010) Key features of the IPSL ocean atmosphere model and its sensitivity to atmospheric resolution. Clim Dyn 34:1–26

Mecking JV, Keenlyside NS, Greatbatch RJ (2013) Stochastically-forced multidecadal variability in the North Atlantic: a model study. Clim Dyn. doi:10.1007/s00382-013-1930-6

Medhaug I, Furevik T (2011) North Atlantic 20th century multidecadal variability in coupled climate models: sea surface temperature and ocean overturning circulation. Ocean Sci 7:389–404

Medhaug I, Langehaug RH, Eldevik T, Furevik T, Bentsen M (2012) Mechanisms for decadal scale variability in a simulated Atlantic meridional overturning circulation. Clim Dyn 39:77–93

Menary BM, Park W, Lohmann K, Vellinga M, Palmer MD, Latif M, Jungclaus JH (2012) A multimodel comparison of centennial Atlantic meridonal overturning circulation variability. Clim Dyn 38:2377–2388

Oka A, Hasumi H, Okada N, Sakamoto TT, Suzuki T (2006) Deep convection seesaw controlled by freshwater transport through the Denmark Strait. Ocean Model 15:157–176

Otterå OH, Bentsen M, Bethke I, Kvamstø NG (2009) Simulated pre-industrial climate in Bergen Climate Model (version 2): model description and large-scale circulation features. Geosci Model Dev 2:197–212

Otterå OH, Bentsen M, Drange H, Suo LL (2010) External forcing as a metronome for Atlantic multidecadal variability. Nat Geosci 3:688–694

Park W, Latif M (2010) Pacific and Atlantic multidecadal variability in the Kiel Climate Model. Geophys Res Lett 37:L24702. doi:10.1029/2010GL045560

Park W, Keenlyside NS, Latif M, Stroeh A (2009) Tropical Pacific climate and its response to global warming in the Kiel Climate Model. J Clim 22:71–92

Pickart RS, Straneo F, Moore GWK (2003) Is Labrador Sea water formed in the Irminger Basin? Deep Sea Res Part I 50:23–52

Pohlmann H, Smith DM, Balmaseda MA, Keenlyside NS, MasinaS, Matei D, Müller WA, Rogel P (2013) Predictability of the mid-latitude Atlantic meridional overturning circulation in a multi-model system. Clim Dyn. doi:10.1007/s00382-013-1663-6

Pope V, Gallani M, Rowntree P, Stratton R (2000) The impact of new physical parametrizations in the Hadley Centre Climate Model—HadCM3. Clim Dyn 16:123–146

Randall DA, Wood RA, Bony S, Colman R, Fichefet T, Fyfe J, Kattsov V, Pitman A, Shukla J, Srinivasan J, Stouffer RJ, Sumi A, Taylor KE (2007) Climate models and their evaluation. In: Solomon S, Qin D, Manning M, Chen Z, Marquis M, Averyt KB, Tignor M, Miller HL (eds) Climate change 2007: the physical science basis. contribution of working group I to the fourth assessment report of the intergovernmental panel on climate change. Cambridge University Press, Cambridge, United Kingdom and New York, NY, USA

Schlesinger ME, Ramankutty N (1994) An oscillation in the global climate system of period 65–70 years. Nature 367:723–726

Semenov VA, Latif M, Dommenget D, Keenlyside NS, Strehz A, Martin T, Park W (2010) The impact of North Atlantic-Arctic multidecadal variability on northern hemisphere surface air temperature. J Clim 23:5668–5677

Sutton RT, Hodson DLR (2005) Atlantic Ocean forcing of North American and European summer climate. Science 309:115–118

Timmermann A, Latif M, Voss R, Groetzner A (1998) Northern Hemisphere interdecadal variability: a coupled air-sea mode. J Clim 11:1906–1931

Ting MF, Kushnir Y, Seager R, Li CH (2011) Robust feathers of Atlantic multi-decadal variability and its climate impacts. Geophys Res Lett 38:L17705

Vellinga M, Wu P (2004) Low-latitude freshwater influence on centennial variability of the Atlantic thermohaline circulation. J Clim 17(23):4498–4511

Visbeck M, Cullen H, Krahmann G, Naik N (1998) An ocean model's response to North Atlantic Oscillation-like wink forcing. Geophys Res Lett 25:4521–4525

Voldoire A, Sanchez-Gomez E, Salas y Mélia D, Decharme B, Cassou C, Sénési S, Valcke S, Beau I, Alias A, Chevallier M, Déqué M, Deshayes J, Douville H, Fernandez E, Madec G, Maisonnave E, Moine MP, Planton S, Saint-Martin D, Szopa S, Tyteca S, Alkama R, Belamari S, Braun A, Coquart L, Chauvin F (2013) The CNRM-CM5.1 global climate model: description and basic evaluation. Clim Dyn 40(9–10):2091–2121. doi:10.1007/s00382-011-1259-y

Volodin EM, Dianskii NA, Gusev AV (2010) Simulation present day climate with the INMCM4.0 coupled model of the atmospheric and oceanic general circulations Izvestia RAS. Atmos Ocean Phys 46:414–431

Wouters B, Drijfhout S, Hazeleger W (2012) Interdecadal North-Atlantic meridional overturning circulation variability in EC-EARTH. Clim Dyn 39(11):2695–2712

Yeager S, Karspeck A, Danabasoglu G, Tribbia J, Teng H (2012) A decadal prediction case study: late 20th century North Atlantic Ocean heat content. J Clim 25:5173–5189. doi:10.1175/JCLI-D-11-00595.1

Zhang R (2010) Latitudinal dependence of Atlantic meridional overturning ciruclation (AMOC) variations. Geophys Res Lett 37:L16703. doi:10.1029/2010GL044474

Zhang R, Delworth TL (2006) Impact of Atlantic multidecadal oscillations on India/Sahel rainfall and Atlantic hurricanes. Geophys Res Lett 33:L17712

Zhang L, Wang C (2013) Multidecadal North Atlantic sea surface temperature and Atlantic meridional overturning circulation variability in CMIP5 historical simulations. J Geophys Res Oceans 118:5772–5791. doi:10.1002/jgrc.20390

Zhang R, Delworth TL, Held IM (2007) Can the Atlantic Ocean drive the observed multidecadal variability in Northern Hemisphere mean temperature? Geophys Res Lett 34:L02709

Zhang R, Delworth TL, Sutton R, Hodson D, Dixon KW, Held IM, Kushnir Y, Marshall D, Ming Y, Msadek R, Robson J, Rosati A, Ting MF, GA (2013) Have aerosols caused the observed atlantic multidecadal variability? J Atmos Sci, 70(4). doi:10.1175/JAS-D-12-0331.1